Transcription factor POU3F2 regulates *TRIM8* expression contributing to cellular functions implicated in schizophrenia

Chaodong Ding[1,2], **Chunling Zhang**[3], **Richard Kopp**[2], **Liz Kuney**[2], **Qingtuan Meng**[1,4,5], **Le Wang**[1,6], **Yan Xia**[1,2], **Yi Jiang**[1,7], **Rujia Dai**[2], **Shishi Min**[1,2], **Wei-Dong Yao**[2], **Ma-Li Wong**[2], **Hongyu Ruan**[2,*], **Chunyu Liu**[1,2,8,*], **Chao Chen**[1,9,10,11,*]

[1]Center for Medical Genetics and Hunan Key Laboratory of Medical Genetics, School of Life Sciences, Central South University, Changsha, Hunan, China

[2]Department of Psychiatry, State University of New York Upstate Medical University, Syracuse, NY, USA

[3]Department of Neuroscience and Physiology, State University of New York Upstate Medical University, Syracuse, NY, USA

[4]Guangxi Clinical Research Center for Neurological Diseases, Affiliated Hospital of Guilin Medical University, Guilin, Guangxi, China

[5]Guangxi Key Laboratory of Brain and Cognitive Neuroscience, Guilin Medical University, Guilin, Guangxi, China

[6]Child Health Institute of New Jersey, Department of Neuroscience and Cell Biology, Rutgers-Robert Wood Johnson Medical School, New Brunswick, NJ, USA

[7]Department of Molecular Physiology and Biophysics, Vanderbilt University, Nashville, TN, USA

[8]School of Psychology, Shaanxi Normal University, Xi'an, Shaanxi, China

[9]National Clinical Research Center for Geriatric Disorders, the Xiangya Hospital, Central South University, Changsha, Hunan, China

[10]Hunan Key Laboratory of Animal Models for Human Diseases, Central South University, Changsha, Hunan, China

[11]Hunan Key Laboratory of Molecular Precision Medicine, Central South University, Changsha, Hunan, China

Abstract

*Corresponding author. liuch@upstate.edu (C.L.); chenchao@sklmg.edu.cn (C.C.); RuanH@upstate.edu (H.R.).

Conflict of interest: The authors declare that they have no conflicts of interest.

Schizophrenia (SCZ) is a neuropsychiatric disorder with aberrant expression of multiple genes. However, identifying its exact causal genes remains a considerable challenge. The brain-specific transcription factor POU3F2 (POU domain, class 3, transcription factor 2) has been recognized as a risk factor for SCZ, but our understanding of its target genes and pathogenic mechanisms are still limited. Here we report that *POU3F2* regulates 42 SCZ-related genes in knockdown and RNA sequencing experiments of human neural progenitor cells (NPCs). Among those SCZ-related genes, *TRIM8* (Tripartite motif containing 8) is located in SCZ-associated genetic locus and is aberrantly expressed in patients with SCZ. Luciferase reporter and electrophoretic mobility shift assays (EMSA) showed that POU3F2 induces *TRIM8* expression by binding to the SCZ-associated SNP (single nucleotide polymorphism) rs5011218, which affects POU3F2 binding efficiency at the promoter region of *TRIM8*. We investigated the cellular functions of *POU3F2* and *TRIM8* as they co-regulate several pathways related to neural development and synaptic function. Knocking down either *POU3F2* or *TRIM8* promoted the proliferation of NPCs, inhibited their neuronal differentiation, and impaired the excitatory synaptic transmission of NPC-derived neurons. These results indicate that *POU3F2* regulates *TRIM8* expression through the SCZ-associated SNP rs5011218, and both genes may be involved in the etiology of SCZ by regulating neural development and synaptic function.

Introduction

Schizophrenia (SCZ) is a highly heritable psychiatric disorder with complex pathogenic mechanisms that are not fully understood[1]. Several leading hypotheses have been aimed at its etiology. Two of these are based upon the disruption of neural development and synaptic function, proposing that abnormal neural structure, function, and connectivity are at fault[2, 3]. Genetic studies also support such theories, associating SCZ with widespread gene dysregulations. Indeed, large scale genome-wide association studies (GWAS) have identified hundreds of genes linked to SCZ[4]. Dozens of these SCZ-related genes, such as *GLT8D1*, *MiR-137*, and *CACNA1C*, affect neural development and synaptic functions[5–7]. However, for most of these risk genes, little is known about their functional relationship to SCZ and even less about their coordinated function.

SCZ is likely caused by many genes with small effects, but their collective interactions form a functional regulatory network that magnifies their effects considerably[8]. Several regulatory genes act as hub genes regulating their targets within the network, such as transcription factors, microRNAs, and long non-coding RNAs[6, 9, 10]. In a previous study, we constructed a gene coexpression module underlying SCZ risk using 394 brain samples from patients with SCZ and healthy controls[9]. We found brain-specific transcription factor *POU3F2* to be one of the key regulators co-expressed with many genes within the SCZ-related module. *POU3F2* is expressed primarily in the central nervous system and has an essential role in brain development[11]. However, the target genes of *POU3F2* and their relationship with SCZ remain largely unknown.

Findings from several studies support the role of *POU3F2* in SCZ etiology. *POU3F2* involves neuronal functions that favor the neurodevelopmental hypothesis of SCZ. For example, *POU3F2* regulates layer production and cortical neuron migration in the

developing neocortex[11, 12], while *POU3F2*-deficient mice exhibit impaired hippocampal neurogenesis[13]. Further, GWAS and brain imaging analyses have identified SCZ-related brain activity affected by *POU3F2*[14]. Additionally, *POU3F2* expression is found to be aberrantly increased in patients with SCZ in three independent RNA-seq datasets[15]. While such convergent evidence supports *POU3F2* as a contributor to the risk for SCZ, knowledge of the pathogenic mechanism of *POU3F2* is meager. Identifying *POU3F2* targets and associated cellular functions may further clarify its pathogenic mechanism within SCZ.

We hypothesize that *POU3F2* affects neurodevelopment and synaptic functions by regulating its co-expressed genes. To test this hypothesis, we first identified the co-expressed genes of *POU3F2* for those with expression affected by *POU3F2* knockdown in NPCs. Among these *POU3F2* targets, we selected *TRIM8* as a promising SCZ-related gene for downstream studies. *TRIM8* is an E3 ubiquitin ligase and best known for its role in cell proliferation and immune response[16, 17]. To interpret the regulatory mechanisms of POU3F2-regulated *TRIM8* expression, we investigated SCZ GWAS SNPs located in the *TRIM8* promoter region. Lastly, to study the impact of *POU3F2* and *TRIM8* on neural development and synaptic function, we studied several cellular phenotypes associated with the expression changes of *POU3F2* and *TRIM8* in neural cells.

Results

SCZ-related target genes of *POU3F2* identified in NPCs

From a gene coexpression module constructed in our previous study[9], we identified genes whose expression levels were affected by *POU3F2*. The module contained 545 protein-coding genes (Table S1). We wanted to determine if any of these genes were being regulated by *POU3F2* using a cellular model. We first characterized the human induced pluripotent stem cells (iPSCs) and differentiated them into NPCs (Supplementary Fig. 1). Next, we performed *POU3F2* knockdown in the NPCs through lentiviral transduction and observed that 3,421 genes were changed significantly by RNA-seq analysis (false discovery rate (FDR) q < 0.05, Table S2), with 1,961 of them were upregulated and 1,460 were downregulated (Fig. 1A). Of the 3,421 genes with expression changes, 60 overlapped with the 545 module genes and had a consistent direction of alteration in the *POU3F2* knockdown and coexpression analyses (enrichment $P = 9.1e-4$; Fig. 1B, Table S3).

To explore whether these 60 *POU3F2*-regulated genes are also risk genes for SCZ, we examined three published lists of SCZ candidate genes (Table S4) and performed gene enrichment analysis. The first gene list, obtained from the SZDB (schizophrenia database), contained 2,752 genes assembled from the Psychiatric Genomics Consortium (PGC) GWAS study, the sherlock integrative analysis, and a study of genes affected by copy number variations[18]. The second list consisted of 106 genes with SCZ-associated rare variants that were selected from our published study[9]. The third list had 4,096 differentially expressed protein-coding genes from PsychENCODE data (FDR q < 0.05; SCZ n = 559; Control n = 936)[19]. A total of 6,235 SCZ candidate genes resulted from combining these three gene lists. Enrichment analysis identified 42 out of the 60 *POU3F2*-regulated genes from the 6,235 SCZ-related genes (enrichment $P = 2.1e-5$; Fig. 1C, Table S5). Functional enrichment

analysis showed that the 42 genes were significantly enriched in the development of neural cells and the central nervous system (FDR q 0.05; Fig. 1D).

TRIM8 stood out as an SCZ candidate gene among the 42 SCZ-related genes

We prioritized the genes that have been identified as associated with an increased risk for SCZ among the 42 target genes using GWAS and gene expression data. PGC identified *TRIM8*, *NCAN*, and *C1orf54* as SCZ candidate genes in a GWAS study using a cohort of 36,989 cases and 113,075 controls[4]. The other 39 genes were identified in studies of rare variants and differential expression from smaller study samples[9, 19]. *TRIM8*, *NCAN*, and *C1orf54* were selected for further analysis as they were identified in a well-powered study. We found that *TRIM8* was located in the most significant GWAS locus (ranking the third locus, GWAS p = 6.198e-19). *NCAN* and *C1orf54* followed far behind ranking as 47th and 48th loci, respectively (GWAS p = 3.634e-10; p = 4.487e-10). Furthermore, PsychENCODE data showed that *TRIM8* expression increased in the brain tissues of patients with SCZ compared with controls (SCZ n = 559; control n = 936; differential expression p = 0.016), whereas *NCAN* and *C1orf54* expression were not significantly altered[19]. Therefore, we selected *TRIM8* for further study.

Three SCZ SNPs may mediate *POU3F2*-regulated *TRIM8* expression by disrupting POU3F2 binding

Although RNA-seq results showed that *TRIM8* expression decreased after *POU3F2* knockdown, *POU3F2*-specific mechanisms for regulating *TRIM8* expression and its association with SCZ remain unknown. SCZ-related genetic variants are frequently located in non-coding regions, such as in promoter and enhancer regions[20]. These variants regulate gene expression and generate gene expression quantitative trait loci (eQTL)[20]. Furthermore, SCZ-related variants can affect gene expression by disrupting transcription factor binding[21]. Therefore, we hypothesized that SCZ-related variants in the regulatory region of *TRIM8* influence its expression by affecting POU3F2 binding.

To identify the POU3F2 binding-disrupting SNPs associated with *TRIM8* expression, we first identified POU3F2 binding sequences within the 6kb upstream region of *TRIM8* (Table S6), referencing the JASPAR database[22]. We then identified brain eQTL SNPs of *TRIM8* within this 6kb genomic region using Brain eQTL Almanac (BRAINEAC) data from the UK Brain Expression Consortium (Table S7)[23]. Combining these results, we identified two eQTL SNPs (rs5011218 and rs11191359) that were co-localized with the predicted POU3F2 binding sites, and another eQTL SNP (rs4146428) which was near the predicted site (Fig. 2A). Data from the Lieber Institute for Brain Development (LIBD)[24] also confirmed rs5011218 and rs4146428 to be *TRIM8* eQTL signals in the dorsolateral prefrontal cortex (FDR q = 0.0027 for both SNPs, Fig. 2B).

To study the regulatory activity of these three SNPs (rs5011218, rs11191359, and rs4146428), we annotated them using the Encyclopedia of DNA Elements (ENCODE) data as summarized in the University of California Santa Cruz (UCSC) Genome Browser website[25]. Graphical results showed that these three SNPs were covered by H3K27AC and DNaseI hypersensitivity signals, indicating regional high transcriptional activity (Fig. 2C).

We then tested the direct interaction between POU3F2 and the three SNPs. ChIP-seq data from the ENCODE project revealed that POU2F2 binds to the site surrounding rs4146428 in B-lymphocyte cells (Fig. 2C). POU3F2 and POU2F2 have a similar core binding motif within the POU domain. Therefore, POU3F2 could also bind to this site. Considering that POU3F2 is a brain-specific transcription factor and that SCZ-related SNPs confer their effects mainly in the brain, we downloaded POU3F2 ChIP-seq data from NPCs[26]. The analysis revealed ChIP-seq peak signals overlapping these three SNPs sites (Fig. 2C), indicating their direct interaction with the POU3F2 protein.

Finally, we found that the three SNPs described above are associated with SCZ. These three SNPs were included in the PGC-reported set of SCZ GWAS SNPs having a 99% probability of containing SCZ causal variants[4] (rs5011218 GWAS $P = 3.7e-9$, rs11191359 GWAS $P = 2.5e-8$, rs4146428 GWAS $P = 2.8e-8$, Fig. 2A). All three SNPs were in linkage disequilibrium (non-random association of alleles at multiple loci, $r^2 > 0.6$) with the SCZ index SNP rs7907645 (GWAS $P = 1.3e-11$, Fig. 2A). Data from BRAINEAC showed that the index SNP rs7907645 was also an eQTL SNP of *TRIM8* in the occipital cortex ($P = 6.2e-3$, Fig. 2A).

POU3F2 promoted TRIM8 expression, and SNP rs5011218 modulated this regulation by altering POU3F2 binding efficiency

To verify that *POU3F2* positively regulates *TRIM8* expression, we performed transient transfection assays to alter *POU3F2* expression using *POU3F2* overexpression plasmid or small interfering RNA (siRNA). *POU3F2* overexpression in NPCs significantly increased mRNA expression of *TRIM8* (P < 0.01, Fig. 3A) and TRIM8 protein expression (P < 0.01, Fig. 3C). Conversely, *POU3F2* knockdown significantly decreased *TRIM8* mRNA expression (P < 0.001, Fig. 3B) and lowered *TRIM8* protein expression (P < 0.001, Fig. 3D). These results were consistent with the RNA-seq analysis, confirming that *POU3F2* is a positive regulator of *TRIM8* expression in NPCs.

Next, we tested what regulatory effects the different alleles of the three SNPs (rs5011218 A>C, rs11191359 A>T and rs4146428 G>A) have on *TRIM8* expression using the dual-luciferase reporter assay. We first cloned the regulatory element of *TRIM8* containing the reference alleles of three SNPs (rs5011218 A, rs11191359 A, rs4146428 G, Table S8) into luciferase reporter vectors. To see the effects of POU3F2 protein on the activity of the constructed vector, we then co-transfected the reporter vectors and the *POU3F2* overexpression vector into NPCs. The results suggested that POU3F2 significantly increased the luciferase activity of the reporter vector through the regulatory element containing the reference alleles ($P < 0.001$, Fig. 3E). We then mutated the three reference alleles to test the regulatory effects of the alternative alleles. We found that the C allele of rs5011218, the T allele of rs11191359, and the A allele of rs4146428 each significantly inhibited the *POU3F2*-induced upregulation respectively ($P < 0.001$, Fig. 3E).

Finally, we studied the direct interaction between POU3F2 protein and the SNPs using EMSA. While the three SNPs all showed allelic effects in luciferase reporter assays, rs4146428 was not located within the predicted POU3F2 binding sites (Fig. 2A). Therefore, we studied the impact of rs5011218 and rs11191359 on POU3F2 binding by designing

several different probes for EMSA assays (table S9). We observed two shifted bands for rs5011218, suggesting that POU3F2 bound to the designed probes containing either the A or C allele (Fig. 3F). Moreover, POU3F2 protein had higher affinity for the A allele than the C allele. This observation explains the luciferase reporter results for rs5011218, in which the vector carrying allele A showed increased reporter activity. For rs11191359, no direct interaction between POU3F2 protein and the corresponding probes was detected (Supplementary Fig. 2).

POU3F2 and *TRIM8* expressions peaked in the prefrontal cortex during early developmental stages

POU3F2 and *TRIM8* expression patterns were assessed in human tissues using GTEx (genotype-tissue expression) data[27], and we found that both *POU3F2* and *TRIM8* are widely expressed in various brain regions (Supplementary Fig. 3A and Supplementary Fig. 3B). In addition, spatiotemporal expression data from SZDB (schizophrenia database) showed that the mRNA expression levels of *POU3F2* and *TRIM8* gradually increased and then peaked during the early developmental stages of the prefrontal cortex (fetal and infant stages; Supplementary Fig. 3C). These data suggest that *POU3F2* and *TRIM8* may have a role in brain development.

POU3F2 and *TRIM8* co-regulated several signaling pathways associated with neural development and synaptic functions

To further understand the functional roles of *POU3F2* and *TRIM8* implicated in SCZ, we performed pathway enrichment analysis of their co-regulated genes. A total of 1040 genes were significantly changed after *TRIM8* knockdown in NPCs (FDR q < 0.05, Table S10). Genes totaling 600 were upregulated, and 440 downregulated (Supplementary Fig. 4A). When comparing RNA-seq data from *TRIM8* and *POU3F2* knockdown NPCs (Table S10 and Table S2), we found an overlap of 548 genes with consistent alteration direction in the two lists (Supplementary Fig. 4B, Table S11). Compared with the 6235 SCZ-related genes we collected (Table S4), 202 out of the 548 common genes were significantly enriched in the 6,235 SCZ genes (enriched *P* < 0.001, Table S12). The 548 *POU3F2* and *TRIM8* co-regulated genes were used in pathway enrichment analysis by Ingenuity Pathway Analysis (IPA) software. We identified many significantly enriched pathways related to neural development and synaptic functions, such as synaptic long-term depression, Wnt/β-catenin signaling, and axonal guidance signaling (enrichment *P* < 0.05; Supplementary Fig. 4C, Table S13).

POU3F2 and *TRIM8* regulated NPC proliferation by affecting the cell cycle

Based on gene expression pattern and pathway enrichment analysis, we investigated the functional effects of *POU3F2* and *TRIM8* knockdown on cell proliferation. To examine the specificity of our *POU3F2* or *TRIM8* shRNAs, we used three different shRNAs to transfect the NPCs and obtained RNA-seq data from each (Fig. 1A and Supplementary Fig. 4A). We then compared the gene expression signatures produced by these shRNAs, according to the previous study[28]. Pearson correlation analysis showed that the expression levels of each gene from various RNA-seq data were highly correlated (Pearson Correlation Coefficient (PCC) > 0.98, *P* < 0.001; Supplementary Fig. 5). It means that these shRNAs produce the

same gene expression signatures, so the probability of an off-target effect was fairly low since off-target effects are typically random and are not reproducible. We then selected one of the shRNAs to knock down *POU3F2* and *TRIM8* expression, independently, in NPCs. Lentivirus encoding shRNA against *POU3F2* (sh*POU3F2*-C) significantly decreased endogenous *POU3F2* expression, and *TRIM8* expression was also significantly decreased (respectively by 51%, $P < 0.001$ and by 43%, $P < 0.001$; Fig. 4A and 4B). However, *TRIM8* shRNA (sh*TRIM8*-C) decreased *TRIM8* expression by 59% ($P < 0.001$; Fig. 4B) but had no effect on *POU3F2* expression ($P > 0.05$; Fig. 4A). We also significantly upregulated *TRIM8* expression in the *POU3F2* knockdown cell line to determine if we could functionally rescue the phenotype changes in *POU3F2* knockdown cells. (*TRIM8* increased by 51%, $P < 0.001$; Fig. 4B).

We then studied the effects of expression changes of *POU3F2* and *TRIM8* on cell proliferation using EdU (5-ethynyl-2'-deoxyuridine) staining and CCK-8 (cell counting kit-8). With EdU staining, *POU3F2* and *TRIM8* knockdown significantly increased the ratio of EdU-positive cells (dividing cells) compared to control, respectively (increased by 39.8% and 36%, respectively, $P < 0.001$ for both; Fig. 4C and 4D). We also observed that *TRIM8* overexpression reversed the increased ratio, induced by *POU3F2* knockdown (decreased by 31.5%, $P < 0.001$; Fig. 4C and 4D). With the CCK-8 assay, we observed that silencing *POU3F2* or *TRIM8* increased the number of cells significantly at day 5 ($P < 0.001$; Fig. 4E), and overexpressing *TRIM8* produced the opposite effect in *POU3F2* knockdown NPCs ($P < 0.01$; Fig. 4E). Here we also performed the CCK-8 assay in another NPC line from StemCell Technologies. The result of this clone was the same. *POU3F2* and *TRIM8* knockdown significantly increased the number of cells at day 5, and *TRIM8* overexpression reversed the proliferation rate in *POU3F2* knockdown NPCs ($P < 0.001$; Supplementary Fig. 6).

To study how *POU3F2* and *TRIM8* knockdown promote cell proliferation, we performed cell cycle analyses. Flow cytometric analysis showed that *POU3F2* or *TRIM8* knockdown significantly decreased the proportion of NPCs in G1 phase respectively, compared with the control ($P < 0.001$ for both, Fig. 4F and 4G). In contrast, the proportion of cells in S and G2 phases significantly increased after reducing *POU3F2* or *TRIM8* expression in NPCs ($P < 0.001$ for both, Fig. 4F and 4G). These suggest that *POU3F2* and *TRIM8* knockdown promote cell transition from the G1 phase to the S and G2 phases. Finally, we found that *TRIM8* overexpression in *POU3F2* knockdown cells significantly reversed the cell proportion of each phase ($P < 0.001$, Fig. 4F and 4G).

To exclude the possibility of off-target effects on NPC proliferation for the shRNA lentivirus (sh*POU3F2*-C and sh*TRIM8*-C), we used additional lentivirus sh*POU3F2*-B and sh*TRIM8*-B to study the functional effects of *POU3F2* and *TRIM8* on cell proliferation. The results for sh*POU3F2*-B and sh*TRIM8*-B lentivirus were consistent with the original lentivirus. The sh*POU3F2*-B and sh*TRIM8*-B lentivirus significantly reduced the expressions of *POU3F2* and *TRIM8* compared with controls (decreased by 54% and 49%, respectively, $P < 0.001$ for both; Supplementary Fig. 7A and 7B). With EdU staining, EdU-positive cells were significantly increased in *POU3F2* and *TRIM8* knockdown NPCs compared with controls (increased by 41% and 33%, respectively, $P < 0.01$ for both; Supplementary Fig. 7C and 7D). With the CCK-8 assay, silencing *POU3F2* or *TRIM8* increased the number of cells

significantly at day 5 ($P < 0.001$; Supplementary Fig. 7E). Cell cycle analysis showed that *POU3F2* and *TRIM8* knockdown both significantly decreased the proportion of NPCs in G1 phase, compared with the control ($P < 0.001$, Supplementary Fig. 7F and 7G). The proportion of cells in S and G2 phases significantly increased after reducing *POU3F2* or *TRIM8* expression in NPCs ($P < 0.01$ for both, Supplementary Fig. 7F and 7G). Finally, we found that *TRIM8* overexpression in *POU3F2* knockdown NPCs significantly reversed each cellular phenotype ($P < 0.01$, Supplementary Fig. 7).

POU3F2 and *TRIM8* regulated the neuronal differentiation and excitatory synaptic transmission

We tested the effects of *POU3F2* and *TRIM8* on the differentiation of NPCs to neurons and astrocytes. Compared to controls cells, *POU3F2* or *TRIM8* knockdown in NPCs significantly reduced the ratio of Tuj1 (Neuron specific class III beta-tubulin, immature neurons marker)-positive neurons (for *POU3F2*, $P < 0.01$; for *TRIM8*, $P < 0.001$; Fig. 5A and 5B). *TRIM8* overexpression rescued the differentiation defect of *POU3F2* knockdown NPCs, as confirmed by significantly increased Tuj1-positive neurons ($P < 0.01$; Fig. 5A and 5B). Unexpectedly, *POU3F2* and *TRIM8* knockdown did not affect the differentiation of NPCs into astrocytes (Supplementary Fig. 8A and 8B). We quantified the number and length of neuronal dendrites after differentiating NPCs into mature neurons. Dendrite length and number were significantly decreased in neurons with lower *POU3F2* or *TRIM8* expression (for *POU3F2*, $P < 0.001$ for length and number; for *TRIM8*, $P < 0.01$ for length and $P < 0.001$ for number; Fig. 5C, 5D and 5E). Dendrite length and number in *POU3F2* knockdown neurons were rescued by *TRIM8* overexpression (Fig. 5C, 5D and 5E). We also used another NPC line to study the effects of *POU3F2* and *TRIM8* on neuronal differentiation. This clone also showed that *POU3F2* or *TRIM8* knockdown significantly reduced the ratio of Tuj1-positive neurons, and *TRIM8* overexpression reversed the ratio of Tuj1-positive neurons in *POU3F2* knockdown cells (Supplementary Fig. 8C and 8D).

In addition to neurodevelopmental defects, aberrant expression of SCZ susceptibility genes often causes the dysfunctions of excitatory synaptic transmission of neurons[29, 30]. To examine whether *TRIM8* and *POU3F2* cause this dysfunction, we first differentiated wild type NPCs into mature neurons and then altered the *TRIM8* and *POU3F2* expression in the neurons. We then measured the miniature excitatory postsynaptic currents (mEPSCs), a key indicator of excitatory synaptic transmission. Lentivirus encoding shRNA against *POU3F2* (sh*POU3F2*-C) significantly decreased endogenous *POU3F2* expression, and *TRIM8* expression was also significantly decreased in the mature neurons (respectively by 55%, $P < 0.001$ and by 48%, $P < 0.001$; Supplementary Fig. 9). However, *TRIM8* shRNA (sh*TRIM8*-C) decreased *TRIM8* expression by 58% ($P < 0.001$; Supplementary Fig. 9C) but had no effect on *POU3F2* expression (Supplementary Fig. 9B). We also significantly upregulated *TRIM8* expression in the *POU3F2* knockdown neurons to determine if we could functionally rescue the phenotype changes. (*TRIM8* increased by 42%, $P < 0.001$; Supplementary Fig. 9C). The mEPSCs recorded from *POU3F2* or *TRIM8* knockdown neurons showed a significant decrease in frequency (for *POU3F2*, $P < 0.01$; for *TRIM8*, $P < 0.001$; Fig. 5F and 5G), but no change in amplitude (Fig. 5F, 5H and 5J), compared to controls. The decreased frequency in cells with *POU3F2* and *TRIM8* knockdown is also

revealed with the rightward shift of the cumulative probability curves (Fig. 5I). As expected, *TRIM8* overexpression in *POU3F2* knockdown neurons significantly restored the frequency of mEPSCs ($P < 0.01$; Fig. 5F, and 5G).

To exclude the possibility of off-target effects on neuronal differentiation and synaptic transmission of sh*POU3F2*-C and sh*TRIM8*-C lentivirus, we used sh*POU3F2*-B and sh*TRIM8*-B lentivirus to replicate the functional study. The results of sh*POU3F2*-B and sh*TRIM8*-B lentivirus were consistent with the results of sh*POU3F2*-C and sh*TRIM8*-C. *POU3F2* or *TRIM8* knockdown significantly reduced the ratio of Tuj1-positive neurons ($P < 0.01$ for both; Supplementary Fig. 10A and 10B). Dendritic length and number were significantly decreased in mature neurons with reduced *POU3F2* or *TRIM8* expression ($P < 0.01$; Supplementary Fig. 10C, 10D and 10E). In addition, mEPSCs recorded from *POU3F2* or *TRIM8* knockdown neurons showed a significant decrease in frequency ($P < 0.05$; Supplementary Fig. 10F, 10G, and 10I), without any change in amplitude (Supplementary Fig. 10F, 10H, and 10J), compared with controls. Finally, *TRIM8* overexpression significantly restored each cellular phenotype in the *POU3F2* knockdown cells ($P < 0.05$; Supplementary Fig. 10).

Discussion

Our functional study suggests that *POU3F2* and *TRIM8* are involved in the pathophysiology of SCZ, which is characterized as a disorder of neural development and synaptic function[2, 3]. Focusing on the regulatory mechanisms of *POU3F2*-mediated *TRIM8* expression, we found that two alleles of SCZ-related SNP rs5011218, A and C, showed different binding affinities to POU3F2. The A allele had greater affinity and promoted *TRIM8* expression more effectively than the C allele. PGC reported that patients with SCZ have a significantly higher frequency of the A allele of rs5011218 than healthy controls ($P = 9.65e-9$; SCZ n = 33,426, Control n = 32,541)[31]. Moreover, studies showed that *POU3F2* and *TRIM8* have an abnormally high level of expression in the brain tissue of patients with SCZ[15, 19]. Based on these data, we speculate that both increased expression of *POU3F2* and the rs5011218 A allele aberrantly stimulate high expression of *TRIM8*, which in turn heightens SCZ risk. These results exemplify how non-coding variants can contribute to SCZ risk by affecting gene expression.

POU3F2, *TRIM8*, and their co-regulated genes appear to form a complex regulatory network contributing to SCZ. We observed that *POU3F2* and *TRIM8* co-regulated genes enriched in many established neurodevelopmental and synaptic pathways implicated in SCZ. These pathways include the Wnt/β-catenin, long-term depression (LTD), axonal guidance, and ephrin receptor signaling pathways (Table S13). The Wnt/β-catenin pathway is critical in the formation of neuronal circuits by regulating neuronal differentiation, dendritic development, and synaptic function[32]. SCZ has previously been characterized by dysfunction of Wnt/β-catenin signaling pathway[33]. The LTD pathway is associated with neuronal connectivity by modulating synaptic plasticity[34]. Research shows that patients with SCZ display reduced LTD-like plasticity[35]. The axonal guidance pathway ensures the accurate positioning of axons during synaptic connection and neural circuitry formation[36].

Ephrin receptor signaling is also involved in many neuronal functions, including axonal directional guidance, synaptic plasticity, and cell migration[37].

To elucidate the pathogenic mechanisms of *POU3F2* and *TRIM8,* we studied the cellular functions of the genes using iPSC-derived NPCs and neurons. iPSCs technology and the following neural differentiation methods are useful approaches for the in vitro modeling of SCZ[38]. Many studies show that iPSC-derived NPCs and neurons carrying SCZ-related genetic changes exhibit cellular phenotypes similar to those observed in human postmortem studies and animal models[39–41]. By altering *POU3F2* and *TRIM8* expression, we determined that both regulate NPC proliferation by impacting the cell cycle and that both regulate neuronal differentiation. Abnormalities in cell differentiation and proliferation have been reported in patients with SCZ[42, 43]. Since bipolar disorder is also a neurodevelopmental disorder, and *POU3F2* is located in its genome-wide significant risk locus[44, 45], *POU3F2*-regulated neural functions might also be related to the etiology of bipolar disorder. Moreover, *POU3F2* or *TRIM8* knockdown reduces excitatory synaptic transmission. This similar defect of synaptic function has been observed in postmortem and in vivo studies of patients with SCZ[46–48]. In this way, our study highlights the possible cellular and molecular mechanisms for these phenotypes.

Other published findings also associate *POU3F2* and *TRIM8* with neural development and implicate them in terms of SCZ risk. Children with a mutation in *POU3F2* possess varying degrees of developmental delay and intellectual disability[49, 50]. According to two other studies, children with *TRIM8* mutations also exhibit developmental delays, limited language development, and abnormalities in brain magnetic resonance imaging[51, 52]. *POU3F2* has shown influence over neurogenesis with the regulation of neurodevelopmental genes, such as *Delta1*, *Hes5*, and *Tbr2*[53, 54]. Fibroblasts can be directly differentiated into neurons by *POU3F2* overexpression with a combination of other transcription factors[55]. Santina *et al.* identified several *TRIM8*-regulated neurodevelopmental and synaptic pathways in mouse neural stem cells, such as axonal guidance, ephrin receptor, and synaptic long-term depression pathways[56]. *TRIM8* is an E3 ubiquitin-protein ligase, and this type of ligase plays a key role in the developmental pathogenesis of schizophrenia by regulating synapse plasticity and function[57]. For example, the E3 ligase TRAF6 can affect synaptic transmission by regulating PSD-95 (postsynaptic density protein 95) ubiquitination[58]. These findings support our data showing that *POU3F2* and *TRIM8* regulate neural development and synaptic function. Moreover, *TRIM8* is involved in immune responses by regulating *TNFα* and *IL-1β*[16], and these neurotoxic proinflammatory factors may contribute to brain volume loss in SCZ[59].

There are many interesting genes from the 42 *POU3F2* targeted gene list yet to be studied, including *PAX6* (paired box 6), *NTRK2* (neurotrophic receptor tyrosine kinase 2), *NDRG2* (N-myc downstream-regulated gene 2 protein), and *NCAN* (neurocan core protein). The transcription factor PAX6 has essential functions in early forebrain development[60]. The NTRK2 protein was shown to be a receptor for *BDNF* (brain derived neurotrophic factor) and regulates aspects of neural development, including neurite outgrowth, neuron migration, and synaptic plasticity[61, 62]. *NDRG2* expressed in different brain regions and involved in neurite outgrowth and astrocyte differentiation[63, 64]. Gene *NCAN* is expressed mainly in

nervous system tissue and has effects on cell migration similar to those of *POU3F2*[65]. Therefore, *POU3F2*-regulated target genes may contribute to neurodevelopment in various ways.

Meanwhile, our study bears some limitations. Our validation found only 60 of the 545 genes of the previously constructed coexpression module to be regulated by *POU3F2*. The remainder of *POU3F2* target genes may be missing due to a difference in the cell types and developmental stages used in the two studies. In our previous work, the gene expression data for predicting the *POU3F2* regulatory network was derived from adult brain tissues containing various neural cell types[9], whereas our current study used the early neurodevelopmental cells (NPCs) to validate *POU3F2* regulation. The iPSCs-derived 3D organoids contain multiple neural cell types and can be used to recapitulate complex features of the brain[66]. Therefore, we could select a 3D organoid model to further study gene regulatory relationships and developmental functions. On the other hand, *POU3F2* is only one of the transcription factors in the gene coexpression module, other transcription factors could regulate remaining target genes.

In summary, our study suggests that *POU3F2* and *TRIM8* as risk genes associated with SCZ etiology and SCZ risk variant rs5011218 mediates *POU3F2*-regulated *TRIM8* expression.

Materials and methods

Generation of NPCs and differentiation into neurons and astrocytes

The normal human-induced pluripotent stem cells (iPSCs) were obtained from the ATCC (#ACS-1011) and cultured in mTeSR1 medium (StemCell Technologies, #05850). Human iPSCs were differentiated into NPCs using a neural induction medium (StemCell Technologies, #05835), and NPCs were maintained in Neural Progenitor Medium (StemCell Technologies, #05833). An additional NPC line (StemCell Technologies, #70901) was ordered for cell proliferation and neuronal differentiation assays. Neuronal differentiation was induced by a Neuron Differentiation and Maturation Kit (StemCell Technologies, #08500, #08510). For astrocyte differentiation, NPCs were plated on Matrigel-coated culture dish, then incubated in Astrocyte Differentiation and Maturation media (StemCell Technologies, #08540, #08550).

Karyotyping

The karyotyping was performed as previously described[67]. Cells were treated with colcemid (final concentration 0.1 ug/mL) for 4 hours (h) in 37°C incubator. The cells were harvested using Accutase (StemCell Technologies, #07920) and then incubated with 0.075 M KCl for 10 minutes (min) at 37°C. Cells were then treated with Carnoy fixative. metaphase spreads were prepared from cells using the airdrying method, followed by the protocol for G binding using Giemsa stain. The number and structure of chromosomes were examined in twenty cells.

Lentivirus infection

ShRNA lentiviruses targeting *POU3F2* and *TRIM8* were purchased from Origene (# TL310273V, #TL300821V). The *POU3F2* shRNA lentiviral particles (# TL310273V) contain four specific shRNAs (sh*POU3F2*-A, sh*POU3F2*-B, sh*POU3F2*-C, and sh*POU3F2*-D) and one scrambled shRNA. The *TRIM8* shRNA lentiviral particles (# TL300821V) also contain four specific shRNAs (sh*TRIM8*-A, sh*TRIM8*-B, sh*TRIM8*-C, and sh*TRIM8*-D) and one scrambled shRNA. For RNA-seq analysis, we selected three shRNAs to silence *POU3F2* or *TRIM8* expression in NPCs and used the scrambled shRNA as a negative control. NPCs were infected according to the manufacturer's protocol (MOI=20). After 72 h viral infection, cells were treated with puromycin (1μg/ml) to generate mixed NPCs expressing specific shRNA sequence. The shRNA sequences were as following: sh*POU3F2*-A, 5′-CCTGTATGGCAACGTGTTCTCGCAGACCA-3′; sh*POU3F2*-B, 5′-GGCTCTGGAGAGCCATTTCCTCAAATGCC-3′; sh*POU3F2*-C: 5′-ATGGCGACCGCAGCGTCTAACCACTACAG-3′; sh*TRIM8*-A: 5′-AACCTGAAGCTCACCAACATCGTGGAGAA-3′; sh*TRIM8*-B: 5′-TAAGATCGGCCACCTGAACTCCAAGCTCT-3′; sh*TRIM8*-C: 5′-CGCAAGATTCTCGTCTGTTCTGTGGACAA-3′; scrambled shRNA: 5′-GCACTACCAGAGCTAACTCAGATAGTACT-3′. We selected sh*POU3F2*-C, sh*POU3F2*-B, sh*TRIM8*-C, sh*TRIM8*-B, and the scrambled shRNA to study the functional effects of *POU3F2* and *TRIM8*. Lentiviral ORF (open reading frame) particle of *TRIM8* (Origene, # RC205812L2V) and control lentivirus (Origene, # PS100071V) were used for *TRIM8* overexpression in functional rescue assay.

RNA-seq library preparation and sequencing

Total RNA was extracted from cells using the miRNeasy Mini Kit (217004, Qiagen) and treated with DNAase. The RNA quality was evaluated by Agilent 2100 Bioanalyzer (Agilent Technologies). All samples were of high quality having a RIN index of 10. 450ng RNA per sample was used for library preparation with Illumina TruSeq Stranded Total RNA with Ribo-Zero Gold Kit following manufacturer protocols. Sequencing was performed using an Illumina NextSeq500 sequencer.

RNA-seq data and differential expression analyses

An average of 46M paired-end 75bp reads per sample were generated from sequencing. Raw data in FASTQ format were transferred from the SUNYMAC core facility server. Sequencing quality was accessed by FastQC v0.11.7 program[68], low-quality bases and reads were filtered from raw reads by Trimmomatic v0.36[69] with a Phred score cutoff of 30. The trimmed reads were mapped to Gencode GRCh38.p12 Release 29 human reference genome using STAR aligner v2.6.0c[70]. Reads mapped to genes were summarized by featureCounts program in subread v1.6.1[71]. Genes were filtered by CPM (count-per-million) 1 in at least two samples, and data were normalized to effective library size by edgeR v3.22.3 program. Differential gene expression analyses were performed using edgeR[72]. These RNA-seq data (GSE143692) has been submitted to the GEO (Gene Expression Omnibus) database.

Transient transfection of plasmid and small interfering RNA (siRNA)

The human *POU3F2* overexpression plasmid (pYr-CMV-Kan2-*POU3F2*-Flag) was purchased from Changsha Yingrun Biotechnology (#HO005604). This vector was engineered to express the complete *POU3F2* ORF with an expression flag tag. The corresponding control plasmid (pYr-CMV-Kan2-Flag) was also purchased from Changsha Yingrun Biotechnology (VPY0900). *POU3F2* siRNA was synthesized by Genepharma, with the following sequence: 5′-GGCGGAUCAAACUGGGAUU-3′. The control siRNA sequnece: 5′-UUCUCCGAACGUGUCACGU-3′. For plasmid transfection, cells at 80% confluency in 6-well plates were transfected with 2.5 ug plasmid using Lipofectamine LTX & PLUS Reagent (Invitrogen). For siRNA transfection, cells at 40% confluency in 6-well plates were transfected with siRNA at a final concentration of 50 nmol/L using Lipofectamine RNAiMAX Reagent (Invitrogen). After 36 h, we extracted RNA or protein for expression analyses.

Quantitative Real-time PCR

Total RNA was extracted from cells using the miRNeasy Mini Kit (217004, Qiagen). cDNA was synthesized using the HiScriptII Q Select RT SuperMix (R223–01, Vazyme), after which ChamQ SYBR qPCR Master Mix (Q311–01, Vazyme) was used to quantitate PCR according to the manual. Endogenous housekeeping genes (β-actin or GAPDH) were used as internal standards. The cycling protocol was completed as follows: 30 seconds at 98°C, followed by 35 cycles of 98°C for 15 seconds and 60°C for 30 seconds. The primer sequences are listed in supplementary table S14.

Western Blot

Protein isolation was performed with cell lysis buffer (Beyotime, #P0013). Protein concentration was detected using a Detergent Compatible Bradford Protein Assay Kit (Beyotime). Proteins were separated by SDS-polyacrylamide gel electrophoresis, transferred to PVDF membranes, and blocked by 5% milk for 1.5 h. Membranes were incubated with primary antibodies overnight at 4°C. The following antibodies were used: POU3F2 (1:1000, Cell Signaling Technology 12137), TRIM8 (1:1000, Abcam ab155674), and GAPDH (1:10000, Sigma G9295). Corresponding secondary antibodies (1:5000, Jackson ImmunoResearch 111–035-144) were used to bind with primary antibodies at room temperature for 2 h. Protein bands were detected by chemiluminescence using the BeyoECL Plus (Beyotime, #P0018S). Relative intensities of the protein bands were quantified by software ImageJ (https://imagej.nih.gov/ij/).

Immunocytochemistry

After washing twice with PBS, cells were fixed with 4% formaldehyde for 15 min and permeabilized with 0.1% Triton X-100 for 10 min at room temperature. After washing thrice with PBS, cells were blocked in PBS containing 5% BSA for 30 min, followed by incubation with primary antibodies for 1.5 h at room temperature. Primary antibodies were as follows: Pax6 (1:100, Santa Cruz sc-32766), Nestin (1:100, Santa Cruz sc-23927), Nanog (1:200, Cell Signaling Technology 4903), OCT4 (1:200, Cell Signaling Technology 2750), Tuj1(1:200, Cell Signaling Technology 5568), MAP2 (1:200, Cell Signaling Technology

8707), and GFAP (1:200, Cell Signaling Technology 3670). After washing twice with PBS, cells were incubated with fluorescence-labeled secondary antibodies (1:200, Jackson ImmunoResearch 115–165-003 and 115–545-003) for 1 h at room temperature. Finally, 1 ug/ml DAPI was used for staining the nuclei.

Prediction of POU3F2 binding sites and regulatory SNPs

To identify POU3F2 binding sites and regulatory SNPs located within the regulatory region of *TRIM8*, we downloaded the 6kb upstream regulatory sequences of *TRIM8* from the UCSC website[25]. After this, we predicted putative POU3F2 binding sites from these data using the JASPAR database[22]. The relative profile score threshold was 60%. For regulatory SNPs prediction, we collected all SNPs within the 6kb upstream region of *TRIM8* using the UCSC website. Among these SNPs, eQTL SNPs of *TRIM8* were selected for further analysis using the BRAINEAC database[23].

Dual-luciferase reporter assay

The upstream regulatory region containing the reference alleles of three SNPs (rs5011218, rs11191359, and rs4146428) was cloned into the PGL3-Basic vector using a One Step Cloning Kit (Vazyme, C112). This region is 1003 bp and contains the A alleles of rs5011218 and rs11191359 and G allele of rs4146428. The sequence and SNPs information are listed in table S8. The Fast Mutagenesis Kit V2 (Vazyme, C214) was used for SNP mutation. NPCs were co-transfected with 500 ng reconstructed vector, 10 ng pRL-TK, and 500 ng *POU3F2* overexpression vectors (or empty vectors) in 24-well plates. After 48 h, the activities of firefly luciferase and renilla luciferase were measured using the dual-luciferase assay kit (Promega, E1910).

Electrophoretic mobility shift assay

After transient transfection with the *POU3F2* overexpression vector for 48 h, nuclear proteins were extracted from NPCs using NE-PER nuclear reagents (Thermo scientific, 78833). Oligonucleotide probes were designed with corresponding SNPs, flanked by 15 bp, in both a cold and 5′ biotinylated form (supplementary table S9). Oligonucleotides were annealed by heating to 95°C for 5 min with subsequent cooling to room temperature (5°C/min). POU3F2 antibody (Santa Cruz, sc-393324X) was used to achieve gel supershift. EMSA was performed with Light Shift Chemiluminescent EMSA Kit (Thermo scientific, 20148). The binding reaction was carried out at 25°C for 30 min with 6 ug of nuclear extract and 20 fmol of labeled probes. The samples were electrophoresed in a 6% polyacrylamide gel at 100 V until the bromophenol migrated approximately 3/4 down the length of the gel. The transfer was completed 200mA for 1.5 h. When the transfer was completed, the transferred DNA was crosslinked to a nylon membrane. Finally, biotin-labeled DNA was detected by chemiluminescence.

NPCs proliferation assay

Cell proliferation was assessed using cell counting kit-8 (Beyotime, C0038) and BeyoClick™ EdU cell proliferation kit (Beyotime, C0075L). For the cell counting kit-8 assay, 2×10^3 NPCs were seeded into 96-well plates, initially. At various later time points,

20ul WST-8 was added into each well, which contained 200 ul of media. The plates were then incubated at 37°C for 4 h before the optical density was measured at 450 nm in a microplate reader (BioTek). For the EdU staining assay, 1×10^6 NPCs were plated on 25mm coverslips and cultured overnight. Next, we removed half of the medium volume and added an equal volume of the EdU working solution (20uM) to make a final concentration of 10uM. After incubating for 5 h, we used 4% formaldehyde for cell fixation and 0.3% TritonX-100 for permeabilization. Finally, we performed the EdU detection and DNA staining using click additive solution and Hoechst 33342.

Cell cycle analysis

We used the cell cycle analysis kit (Beyotime, C1052) for cell staining. Cells were briefly washed twice in 1X PBS before being fixed overnight in 70% ethanol. On the following day, cells were stained with a solution of propidium iodide (PI) at 37°C for 30 min after being washed three times with 1X PBS. Finally, the cells were analyzed using FACScalibur (BD Biosciences).

Quantification of dendritic length and number

Neurons were stained with MAP2 for dendritic length and number measurements. We used the NeuronJ program to trace dendrites following the instructions[73]. Dendrites were assigned to clusters, with each cluster comprised of a primary dendrite and all its associated branches. After tracing was completed and clusters were assigned, a text file containing the dendritic length and number information was generated. A total of 64 neurons were measured for each group.

Electrophysiological recordings

We seeded NPCs onto glass coverslips and differentiated them into neurons for 50 days using a Neuron Differentiation and Maturation Kit (StemCell Technologies, #08500, #08510) for electrophysiological recordings. We then used the purchased lentivirus (sh*POU3F2*-C, sh*TRIM8*-C, and scrambled shRNA, MOI=20) to alter the gene expression in the neurons, after which we cultured the neurons for 5 additional days before whole-cell patch-clamp recordings as previously described[58]. At room temperature, mEPSCs were recorded at −60 mV. The pipettes were filled with solutions containing (in mM): 130 K-gluconate, 8 NaCl, 10 HEPES, 0.4 EGTA, 2 Mg-ATP, and 0.25 GTP-Tris, pH 7.25. During the recording, neurons were maintained in the artificial cerebrospinal fluid (ACSF) bubbled with a mixture of CO2 (5%) and O2 (95%). The ACSF contained (in mM): 121 NaCl, 4.2 KCl, 1.1 CaCl2, 1 MgSO4, 29 NaHCO3, 0.45 NaH2PO4-H2O, 0.5 Na2HPO4, and 20 glucose. Picrotoxin (PTX, 100uM) and tetrodotoxin (TTX, 1 μM) were added to the ACSF to block GABAAA receptor-mediated inhibitory responses and action potential-evoked synaptic responses, respectively. The Multiclamp 200B and pCLAMP software (Molecular Devices) were used for signal recording. Data were analyzed by Clampfit 10.7 and Mini Analysis softwares.

Statistical Analysis

Data are expressed as mean ± standard deviation (SD) with statistical comparisons performed using Student's t-test. Results were considered statistically significant at p<0.05. P values were adjusted for multiple testing using the Benjamini-Hochberg method. We used Fisher's exact test or Chi-square test to assess the significance of gene enrichment analysis, and image fields were randomly selected under 20X or 40X magnification.

URLs

For JASPAR database[22], http://jaspar.genereg.net/; For BRAINEAC data[23], http://www.braineac.org/; For LIBD database[24], http://eqtl.brainseq.org/phase1/eqtl/; For UCSC Genome Browser[25], https://genome.ucsc.edu; For GTEx[27], https://gtexportal.org/; For SZDB[18], http://www.szdb.org/index.html;

Supplementary Material

Refer to Web version on PubMed Central for supplementary material.

Acknowledgments

References

1. Walker E, Kestler L, Bollini A, Hochman KM. Schizophrenia: etiology and course. Annu Rev Psychol 2004; 55: 401–430. [PubMed: 14744221]

2. Frankle WG, Lerma J, Laruelle M. The Synaptic Hypothesis of Schizophrenia. Neuron 2003; 39(2): 205–216. [PubMed: 12873379]

3. Birnbaum R, Weinberger DR. Genetic insights into the neurodevelopmental origins of schizophrenia. Nat Rev Neurosci 2017; 18(12): 727–740. [PubMed: 29070826]

4. Schizophrenia Working Group of the Psychiatric Genomics C. Biological insights from 108 schizophrenia-associated genetic loci. Nature 2014; 511(7510): 421–427. [PubMed: 25056061]

5. Yang CP, Li X, Wu Y, Shen Q, Zeng Y, Xiong Q et al. Comprehensive integrative analyses identify GLT8D1 and CSNK2B as schizophrenia risk genes. Nat Commun 2018; 9(1): 838. [PubMed: 29483533]

6. Yin J, Lin J, Luo X, Chen Y, Li Z, Ma G et al. miR-137: a new player in schizophrenia. Int J Mol Sci 2014; 15(2): 3262–3271. [PubMed: 24566148]

7. Simms BA, Zamponi GW. Neuronal voltage-gated calcium channels: structure, function, and dysfunction. Neuron 2014; 82(1): 24–45. [PubMed: 24698266]

8. Fromer M, Roussos P, Sieberts SK, Johnson JS, Kavanagh DH, Perumal TM et al. Gene expression elucidates functional impact of polygenic risk for schizophrenia. Nat Neurosci 2016; 19(11): 1442–1453. [PubMed: 27668389]

9. Chen C, Meng Q, Xia Y, Ding C, Wang L, Dai R et al. The transcription factor POU3F2 regulates a gene coexpression network in brain tissue from patients with psychiatric disorders. Sci Transl Med 2018; 10(472): eaat8178. [PubMed: 30545964]

10. Ren Y, Cui Y, Li X, Wang B, Na L, Shi J et al. A co-expression network analysis reveals lncRNA abnormalities in peripheral blood in early-onset schizophrenia. Prog Neuropsychopharmacol Biol Psychiatry 2015; 63: 1–5. [PubMed: 25967042]

11. He X, Treacy M, Simmons D, Ingraham H, Swanson L, Rosenfeld M. Expression of a large family of POU-domain regulatory genes in mammalian brain development. Nature 1989; 340(6228): 35–41. [PubMed: 2739723]

12. McEvilly R, de DM, Schonemann M, Hooshmand F, Rosenfeld M. Transcriptional regulation of cortical neuron migration by POU domain factors. Science 2002; 295(5559): 1528–1532. [PubMed: 11859196]

13. Hashizume K, Yamanaka M, Ueda S. POU3F2 participates in cognitive function and adult hippocampal neurogenesis via mammalian-characteristic amino acid repeats. Genes Brain Behav 2018; 17(2): 118–125. [PubMed: 28782255]

14. Potkin SG, Turner JA, Guffanti G, Lakatos A, Fallon JH, Nguyen DD et al. A genome-wide association study of schizophrenia using brain activation as a quantitative phenotype. Schizophr Bull 2009; 35(1): 96–108. [PubMed: 19023125]

15. Pearl JR, Colantuoni C, Bergey DE, Funk CC, Shannon P, Basu B et al. Genome-Scale Transcriptional Regulatory Network Models of Psychiatric and Neurodegenerative Disorders. Cell Syst 2019; 8(2): 122–135 e127. [PubMed: 30772379]

16. Li Q, Yan J, Mao AP, Li C, Ran Y, Shu HB et al. Tripartite motif 8 (TRIM8) modulates TNFalpha- and IL-1beta-triggered NF-kappaB activation by targeting TAK1 for K63-linked polyubiquitination. Proc Natl Acad Sci U S A 2011; 108(48): 19341–19346. [PubMed: 22084099]

17. Caratozzolo MF, Micale L, Turturo MG, Cornacchia S, Fusco C, Marzano F et al. TRIM8 modulates p53 activity to dictate cell cycle arrest. Cell Cycle 2012; 11(3): 511–523. [PubMed: 22262183]

18. Wu Y, Yao YG, Luo XJ. SZDB: A Database for Schizophrenia Genetic Research. Schizophr Bull 2017; 43(2): 459–471. [PubMed: 27451428]

19. Gandal MJ, Zhang P, Hadjimichael E, Walker RL, Chen C, Liu S et al. Transcriptome-wide isoform-level dysregulation in ASD, schizophrenia, and bipolar disorder. Science 2018; 362(6420): eaat8127. [PubMed: 30545856]

20. Roussos P, Mitchell AC, Voloudakis G, Fullard JF, Pothula VM, Tsang J et al. A role for noncoding variation in schizophrenia. Cell Rep 2014; 9(4): 1417–1429. [PubMed: 25453756]

21. Huo Y, Li S, Liu J, Li X, Luo XJ. Functional genomics reveal gene regulatory mechanisms underlying schizophrenia risk. Nat Commun 2019; 10(1): 670. [PubMed: 30737407]

22. Wasserman WW, Sandelin A. Applied bioinformatics for the identification of regulatory elements. Nat Rev Genet 2004; 5(4): 276–287. [PubMed: 15131651]

23. Glass D, Vinuela A, Davies MN, Ramasamy A, Parts L, Knowles D et al. Gene expression changes with age in skin, adipose tissue, blood and brain. Genome Biol 2013; 14(7): R75. [PubMed: 23889843]

24. Jaffe AE, Straub RE, Shin JH, Tao R, Gao Y, Collado-Torres L et al. Developmental and genetic regulation of the human cortex transcriptome illuminate schizophrenia pathogenesis. Nat Neurosci 2018; 21(8): 1117–1125. [PubMed: 30050107]

25. Rosenbloom KR, Sloan CA, Malladi VS, Dreszer TR, Learned K, Kirkup VM et al. ENCODE data in the UCSC Genome Browser: year 5 update. Nucleic Acids Res 2013; 41(Database issue): D56–63. [PubMed: 23193274]

26. Xue Y, Qian H, Hu J, Zhou B, Zhou Y, Hu X et al. Sequential regulatory loops as key gatekeepers for neuronal reprogramming in human cells. Nat Neurosci 2016; 19(6): 807–815. [PubMed: 27110916]

27. Consortium GT. The Genotype-Tissue Expression (GTEx) project. Nat Genet 2013; 45(6): 580–585. [PubMed: 23715323]

28. Semizarov D, Frost L, Sarthy A, Kroeger P, Halbert DN, Fesik SW. Specificity of short interfering RNA determined through gene expression signatures. Proc Natl Acad Sci U S A 2003; 100(11): 6347–6352. [PubMed: 12746500]

29. Cui L, Sun W, Yu M, Li N, Guo L, Gu H et al. Disrupted-in-schizophrenia1 (DISC1) L100P mutation alters synaptic transmission and plasticity in the hippocampus and causes recognition memory deficits. Mol Brain 2016; 9(1): 89. [PubMed: 27729083]

30. Mao W, Watanabe T, Cho S, Frost JL, Truong T, Zhao X et al. Shank1 regulates excitatory synaptic transmission in mouse hippocampal parvalbumin-expressing inhibitory interneurons. Eur J Neurosci 2015; 41(8): 1025–1035. [PubMed: 25816842]

31. Ruderfer DM, Ripke S, McQuillin A, Boocock J, Stahl EA, Pavlides JMW et al. Genomic dissection of bipolar disorder and schizophrenia, including 28 subphenotypes. Cell. 2018;173: 1705–15 [PubMed: 29906448]

32. Rosso SB, Inestrosa NC. WNT signaling in neuronal maturation and synaptogenesis. Front Cell Neurosci 2013; 7: 103. [PubMed: 23847469]

33. Isabella P, Flavia N, Alberto MF, Giorgio D K, Antonio DC, Chiara R et al. Neurodevelopment in Schizophrenia: The Role of the Wnt Pathways. Current Neuropharmacology 2013; 11: 535–558. [PubMed: 24403877]

34. Massey PV, Bashir ZI. Long-term depression: multiple forms and implications for brain function. Trends Neurosci 2007; 30(4): 176–184. [PubMed: 17335914]

35. Hasan A, Nitsche MA, Herrmann M, Schneider-Axmann T, Marshall L, Gruber O et al. Impaired long-term depression in schizophrenia: a cathodal tDCS pilot study. Brain Stimul 2012; 5(4): 475–483. [PubMed: 21945231]

36. Russell SA, Bashaw GJ. Axon guidance pathways and the control of gene expression. Dev Dyn 2018; 247(4): 571–580. [PubMed: 29226467]

37. Klein R, Kania A. Ephrin signalling in the developing nervous system. Curr Opin Neurobiol 2014; 27: 16–24. [PubMed: 24608162]

38. Liu YN, Lu SY, Yao J. Application of induced pluripotent stem cells to understand neurobiological basis of bipolar disorder and schizophrenia. Psychiatry Clin Neurosci 2017; 71(9): 579–599. [PubMed: 28393474]

39. Brennand KJ, Simone A, Jou J, Gelboin-Burkhart C, Tran N, Sangar S et al. Modelling schizophrenia using human induced pluripotent stem cells. Nature 2011; 473(7346): 221–225. [PubMed: 21490598]

40. Yoon K-J, Nguyen Ha N, Ursini G, Zhang F, Kim N-S, Wen Z et al. Modeling a Genetic Risk for Schizophrenia in iPSCs and Mice Reveals Neural Stem Cell Deficits Associated with Adherens Junctions and Polarity. Cell Stem Cell 2014; 15(1): 79–91. [PubMed: 24996170]

41. Habela CW, Song H, Ming GL. Modeling synaptogenesis in schizophrenia and autism using human iPSC derived neurons. Mol Cell Neurosci 2016; 73: 52–62. [PubMed: 26655799]

42. Wang L, Lockstone HE, Guest PC, Levin Y, Palotás A, Pietsch S et al. Expression Profiling of Fibroblasts Identifies Cell Cycle Abnormalities in Schizophrenia. J Proteome Res 2010; 9(1): 521–527. [PubMed: 19916557]

43. Allen KM, Fung SJ, Weickert CS. Cell proliferation is reduced in the hippocampus in schizophrenia. Aust N Z J Psychiatry 2016; 50(5): 473–480. [PubMed: 26113745]

44. Sanches M, Keshavan MS, Brambilla P, Soares JC. Neurodevelopmental basis of bipolar disorder: a critical appraisal. Prog Neuropsychopharmacol Biol Psychiatry 2008; 32(7): 1617–1627. [PubMed: 18538910]

45. Stahl EA, Breen G, Forstner AJ, McQuillin A, Ripke S, Trubetskoy V et al. Genome-wide association study identifies 30 loci associated with bipolar disorder. Nat Genet 2019; 51(5): 793–803. [PubMed: 31043756]

46. Stephan KE, Friston KJ, Frith CD. Dysconnection in schizophrenia: from abnormal synaptic plasticity to failures of self-monitoring. Schizophr Bull 2009; 35(3): 509–527. [PubMed: 19155345]

47. Wong AHC, Van Tol HHM. Schizophrenia: from phenomenology to neurobiology. Neuroscience & Biobehavioral Reviews 2003; 27(3): 269–306. [PubMed: 12788337]

48. Karlsgodt KH, Sun D, Cannon TD. Structural and Functional Brain Abnormalities in Schizophrenia. Curr Dir Psychol Sci 2010; 19(4): 226–231. [PubMed: 25414548]

49. Westphal DS, Riedhammer KM, Kovacs-Nagy R, Meitinger T, Hoefele J, Wagner M. A De Novo Missense Variant in POU3F2 Identified in a Child with Global Developmental Delay. Neuropediatrics 2018; 49(6): 401–404. [PubMed: 30199896]

50. Kasher PR, Schertz KE, Thomas M, Jackson A, Annunziata S, Ballesta-Martinez MJ et al. Small 6q16.1 Deletions Encompassing POU3F2 Cause Susceptibility to Obesity and Variable Developmental Delay with Intellectual Disability. Am J Hum Genet 2016; 98(2): 363–372. [PubMed: 26833329]

51. Assoum M, Lines MA, Elpeleg O, Darmency V, Whiting S, Edvardson S et al. Further delineation of the clinical spectrum of de novo TRIM8 truncating mutations. Am J Med Genet A 2018; 176(11): 2470–2478. [PubMed: 30244534]

52. Sakai Y, Fukai R, Matsushita Y, Miyake N, Saitsu H, Akamine S et al. De Novo Truncating Mutation of TRIM8 Causes Early-Onset Epileptic Encephalopathy. Ann Hum Genet 2016; 80(4): 235–240. [PubMed: 27346735]

53. Dominguez MH, Ayoub AE, Rakic P. POU-III transcription factors (Brn1, Brn2, and Oct6) influence neurogenesis, molecular identity, and migratory destination of upper-layer cells of the cerebral cortex. Cereb Cortex 2013; 23(11): 2632–2643. [PubMed: 22892427]

54. Castro DS, Skowronska-Krawczyk D, Armant O, Donaldson IJ, Parras C, Hunt C et al. Proneural bHLH and Brn proteins coregulate a neurogenic program through cooperative binding to a conserved DNA motif. Dev Cell 2006; 11(6): 831–844. [PubMed: 17141158]

55. Pfisterer U, Kirkeby A, Torper O, Wood J, Nelander J, Dufour A et al. Direct conversion of human fibroblasts to dopaminergic neurons. Proc Natl Acad Sci U S A 2011; 108(25): 10343–10348. [PubMed: 21646515]

56. Venuto S, Castellana S, Monti M, Appolloni I, Fusilli C, Fusco C et al. TRIM8-driven transcriptomic profile of neural stem cells identified glioma-related nodal genes and pathways. Biochim Biophys Acta Gen Subj 2019; 1863(2): 491–501. [PubMed: 30528352]

57. Kohlbrenner EA, Shaskan N, Pietersen CY, Sonntag KC, Woo TW. Gene expression profile associated with postnatal development of pyramidal neurons in the human prefrontal cortex implicates ubiquitin ligase E3 in the pathophysiology of schizophrenia onset. J Psychiatr Res 2018; 102: 110–117. [PubMed: 29635114]

58. Ma Q, Ruan H, Peng L, Zhang M, Gack MU, Yao WD. Proteasome-independent polyubiquitin linkage regulates synapse scaffolding, efficacy, and plasticity. Proc Natl Acad Sci U S A 2017; 114(41): E8760–E8769. [PubMed: 28973854]

59. van Kesteren CF, Gremmels H, de Witte LD, Hol EM, Van Gool AR, Falkai PG et al. Immune involvement in the pathogenesis of schizophrenia: a meta-analysis on postmortem brain studies. Transl Psychiatry 2017; 7(3): e1075. [PubMed: 28350400]

60. Georgala PA, Carr CB, Price DJ. The role of Pax6 in forebrain development. Dev Neurobiol 2011; 71(8): 690–709. [PubMed: 21538923]

61. Zamani A, Xiao J, Turnley AM, Murray SS. Tropomyosin-Related Kinase B (TrkB) Regulates Neurite Outgrowth via a Novel Interaction with Suppressor of Cytokine Signalling 2 (SOCS2). Mol Neurobiol 2019; 56(2): 1262–1275. [PubMed: 29881947]

62. Huang EJ, Reichardt LF. Trk receptors: roles in neuronal signal transduction. Annu Rev Biochem 2003; 72: 609–642. [PubMed: 12676795]

63. Takahashi K, Yamada M, Ohata H, Honda K, Yamada M. Ndrg2 promotes neurite outgrowth of NGF-differentiated PC12 cells. Neurosci Lett 2005; 388(3): 157–162. [PubMed: 16039777]

64. Lin K, Yin A, Yao L, Li Y. N-myc downstream-regulated gene 2 in the nervous system: from expression pattern to function. Acta Biochim Biophys Sin (Shanghai) 2015; 47(10): 761–766. [PubMed: 26341979]

65. Christa K P, Len A P, Kimberly L, Wufang F, Gregory G L. Characterization of the human neurocan gene, CSPG3. Gene 1998; 221: 199–205. [PubMed: 9795216]

66. Logan S, Arzua T, Canfield SG, Seminary ER, Sison SL, Ebert AD et al. Studying Human Neurological Disorders Using Induced Pluripotent Stem Cells: From 2D Monolayer to 3D Organoid and Blood Brain Barrier Models. Compr Physiol 2019; 9(2): 565–611. [PubMed: 30873582]

67. Hu Z, Zhou M, Wu Y, Li Z, Liu X, Wu L et al. ssODN-mediated in-frame deletion with CRISPR/ Cas9 to restore the FVIII function in hemophilia A patient-derived iPSCs and ECs. Mol Ther Nucleic Acids 2019; 17: 198–209. [PubMed: 31261034]

68. Andrews S FastQC: a quality control tool for high throughput sequence data. Babraham Bioinformatics, Babraham Institute, Cambridge, United Kingdom2010.

69. Bolger AM, Lohse M, Usadel B. Trimmomatic: a flexible trimmer for Illumina sequence data. Bioinformatics 2014; 30(15): 2114–2120. [PubMed: 24695404]

70. Dobin A, Davis CA, Schlesinger F, Drenkow J, Zaleski C, Jha S et al. STAR: ultrafast universal RNA-seq aligner. Bioinformatics 2013; 29(1): 15–21. [PubMed: 23104886]

71. Liao Y, Smyth GK, Shi W. featureCounts: an efficient general purpose program for assigning sequence reads to genomic features. Bioinformatics 2013; 30(7): 923–930. [PubMed: 24227677]

72. Robinson MD, McCarthy DJ, Smyth GK. edgeR: a Bioconductor package for differential expression analysis of digital gene expression data. Bioinformatics 2010; 26(1): 139–140. [PubMed: 19910308]

73. Popko J, Fernandes A, Brites D, Lanier LM. Automated analysis of NeuronJ tracing data. Cytometry A 2009; 75(4): 371–376. [PubMed: 18937344]

74. Wang J, Vasaikar S, Shi Z, Greer M, Zhang B. WebGestalt 2017: a more comprehensive, powerful, flexible and interactive gene set enrichment analysis toolkit. Nucleic Acids Res 2017; 45(W1): W130–W137. [PubMed: 28472511]
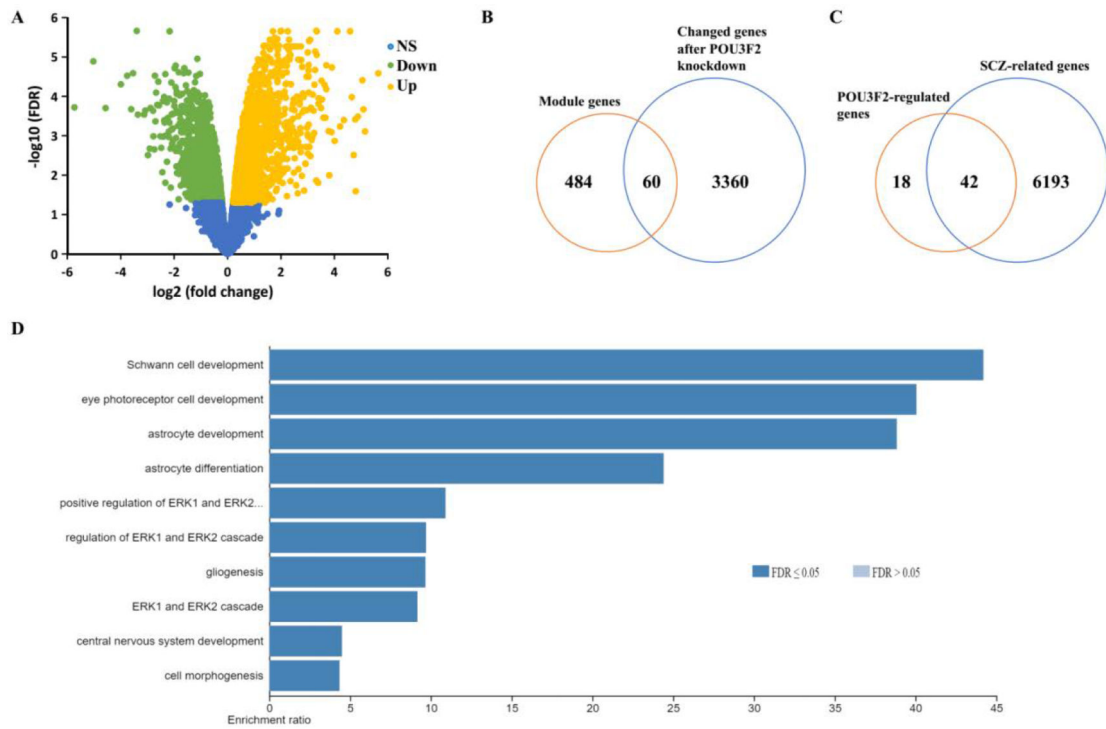
Figure 1. *POU3F2* regulates SCZ-related genes involved in neural development.
(A) Volcano plot of 3,421 differentially expressed genes. NS, not significant; Down, significantly downregulated; Up, significantly upregulated. A total of six samples were analyzed (three *POU3F2* shRNA: sh*POU3F2*-A, sh*POU3F2*-B and sh*POU3F2*-C; three controls). (B) 60 coexpression module genes overlapped with the *POU3F2* knockdown gene list. (C) 42 out of 60 *POU3F2*-regulated genes overlapped with SCZ-related genes. (D) Results of functional enrichment analysis of *POU3F2*-regulated SCZ genes using WebGestalt Toolkit[74].
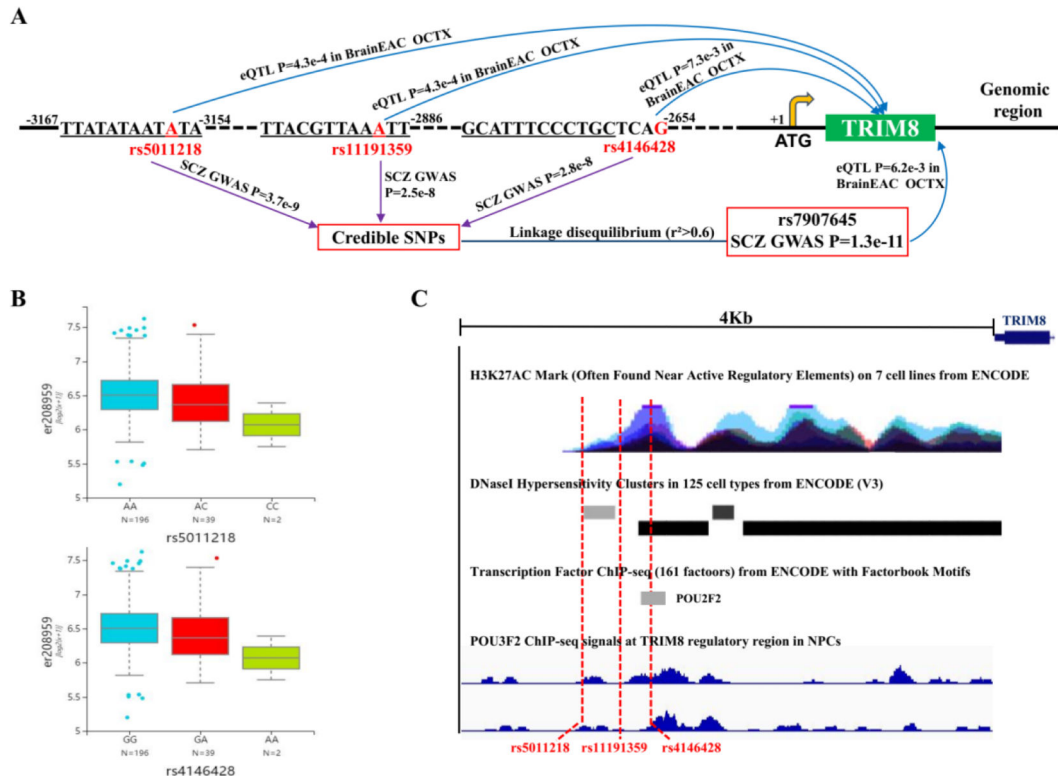
Figure 2. *POU3F2* may affect *TRIM8* expression through three SCZ-related SNPs.
(A) Reference alleles of three SNPs (rs5011218, rs11191359, and rs4146428) are located in the regulatory region of *TRIM8*. The *TRIM8* transcription start site is indicated as +1. Each SNP is marked with an eQTL *P* value and a SCZ GWAS *P* value. OCTX, occipital cortex. (B) LIBD database showed that rs5011218 and rs4146428 are significantly associated with *TRIM8* expression in the dorsolateral prefrontal cortex (FDR q = 0.0027 for both SNPs). These eQTLs were identified using 237 samples. (C) The SNPs were located in upstream regions of *TRIM8* that contains H3K27AC Histone modification, DNase I hypersensitivity and ChIP-seq signals.
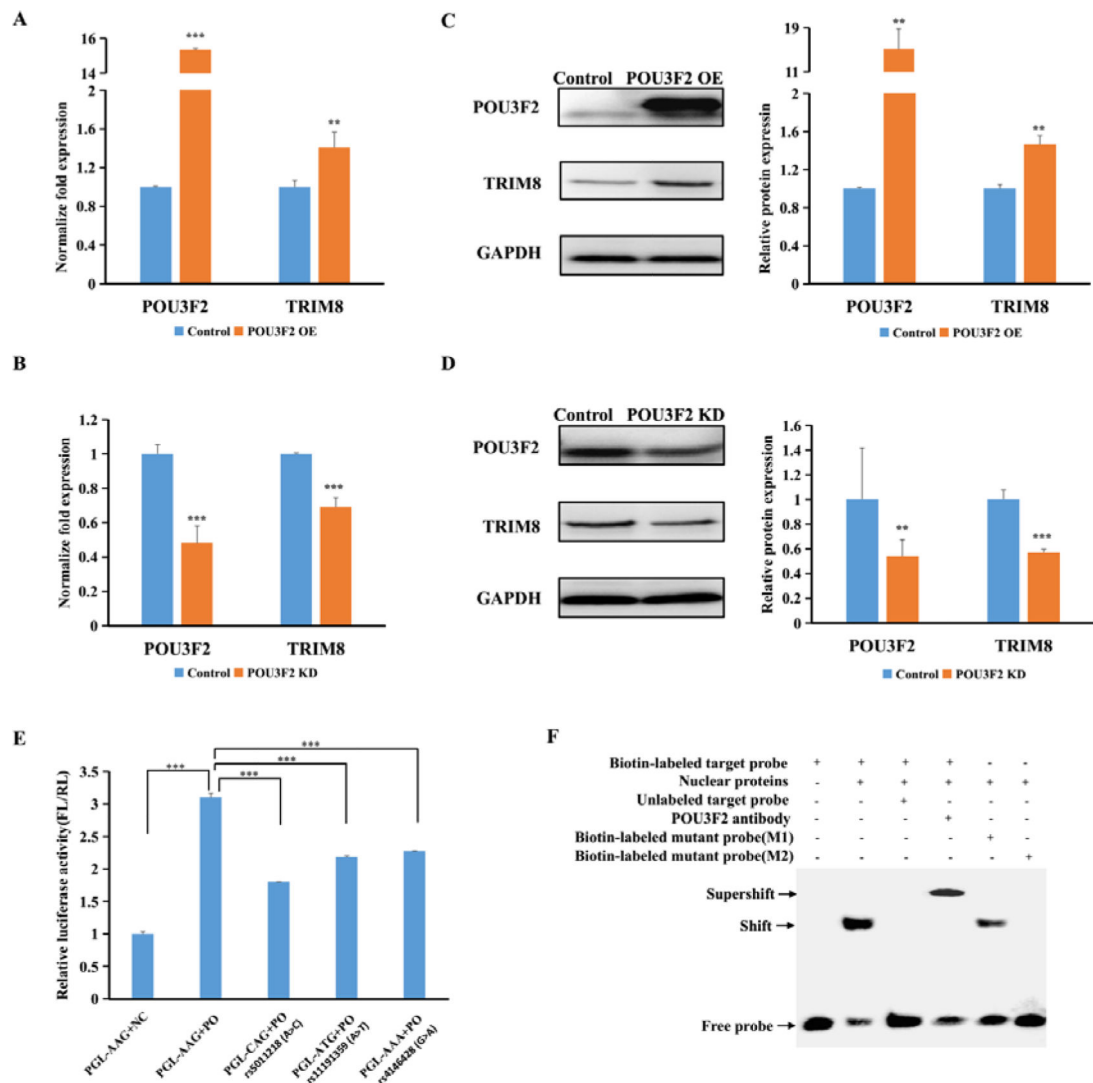
Figure 3. *POU3F2* promoted *TRIM8* expression through the regulatory SNP rs5011218.
(A, B) mRNA expression analyses of *TRIM8* by RT-qPCR after *POU3F2* overexpression
(A) and knockdown (B). Control (A), transfection of control plasmid; *POU3F2* OE,
POU3F2 overexpression, transfection of *POU3F2* overexpression plasmid; Control (B),
transfection of control siRNA; *POU3F2 KD*, *POU3F2* knockdown, transfection of *POU3F2*
siRNA. (C, D) Protein expression analyses of *TRIM8* by Western blotting after *POU3F2*
overexpression (C) and knockdown (D). (E) Luciferase reporter assay of the constructed
vectors. FL, Firefly luciferase; RL, Renilla luciferase; PGL-AAG, luciferase reporter vector
containing the reference alleles of three SNPs; NC, negative control, transfection of control
plasmid; PO, *POU3F2* overexpression, transfection of *POU3F2* overexpression plasmid;
PGL-CAG, the A allele of rs5011218 was mutated into the C allele; PGL-ATG, the A allele
of rs11191359 was mutated into the T allele; PGL-AAA, the G allele of rs4146428 was
mutated into the A allele. N=3 independent biological experiments. For each biological
replicate, we designed three technical replicates. Values represent mean±sd, significance
was determined using Student's t-test. $**P<0.01$, $***P<0.001$. (F) EMSA results of

rs5011218. Lane 1: reaction as the negative control; lane 2: biotin-labeled probes (A allele) plus nuclear proteins; lane 3: excess unlabeled probes displaced binding of biotin-labeled probes; lane 4: anti-POU3F2 antibody combined with protein/DNA complex; lane 5: POU3F2 binding efficiency decreased after the A allele was mutated into C allele; lane 6: binding reaction was totally inhibited after mutating POU3F2 core binding sequences.
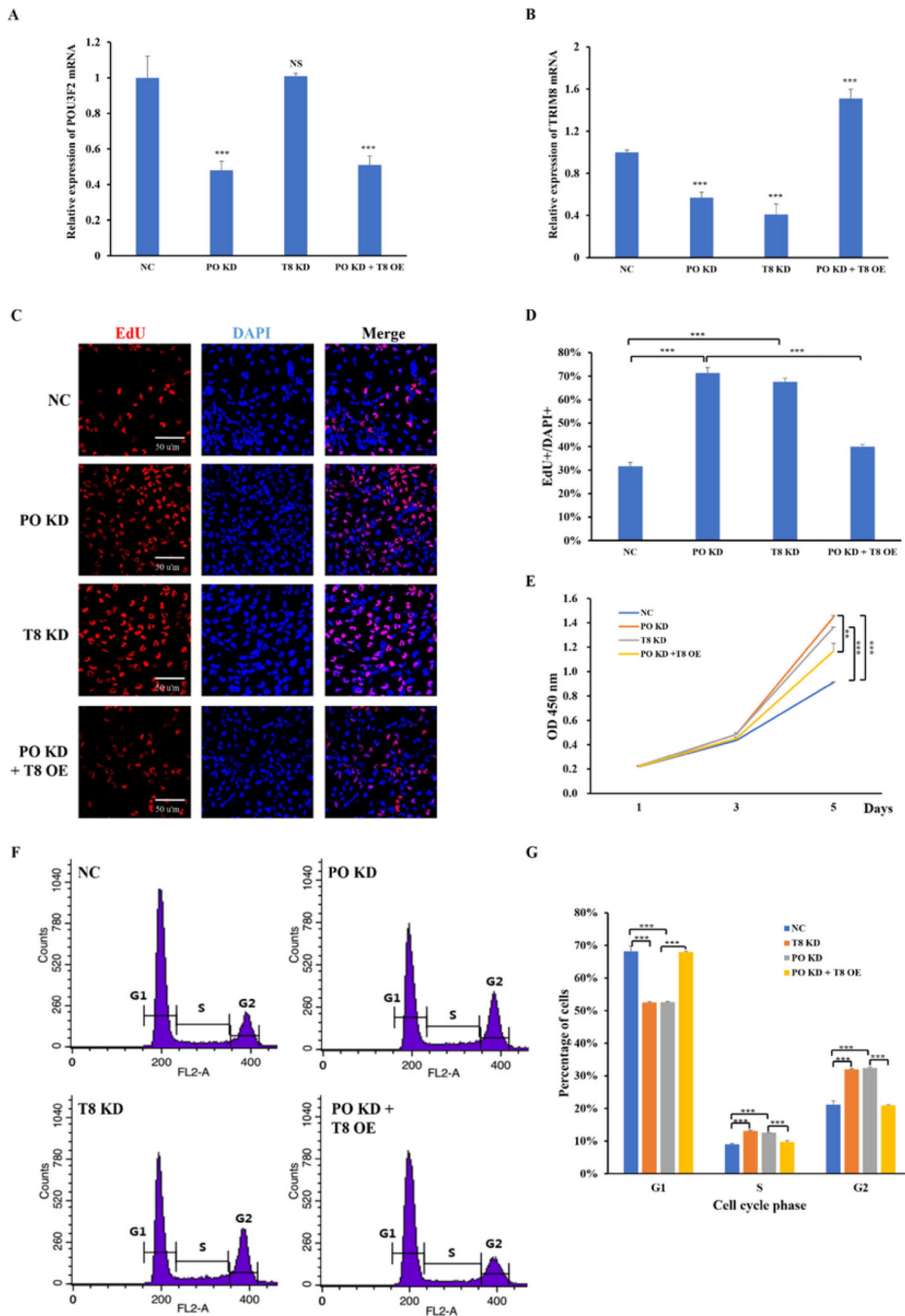
Figure 4. Silencing *POU3F2* and *TRIM8* promote NPCs proliferation through advancing cell cycle progression.

(A) *POU3F2* mRNA expression level in four different cell lines. NC, negative control, infection of scrambled shRNA lentivirus; PO KD, *POU3F2* knockdown, infection of sh*POU3F2*-C lentivirus; T8 KD, *TRIM8* knockdown, infection of sh*TRIM8*-C lentivirus; PO KD + T8 OE, *POU3F2* knockdown plus *TRIM8* overexpression, infection of sh*POU3F2*-C and *TRIM8* overexpression lentivirus; NS, not significant. (B) The mRNA expression level of *TRIM8* in four different cell lines. (C) EdU staining was used to assess the proliferation ability of NPCs after *POU3F2* and *TRIM8* knockdown. (D) Data

quantification for (C). (E) Cell proliferation was evaluated by CCK-8 assay in *POU3F2* and *TRIM8* knockdown cells. (F) Silencing of *POU3F2* and *TRIM8* promoted the cell cycle progression. (G) Data quantification for (F). $**P < 0.01$, $***P < 0.001$. Two-tailed Student's t-test. Values represent the mean±sd from three independent biological replicates. For each biological replicate, we designed three technical replicates.
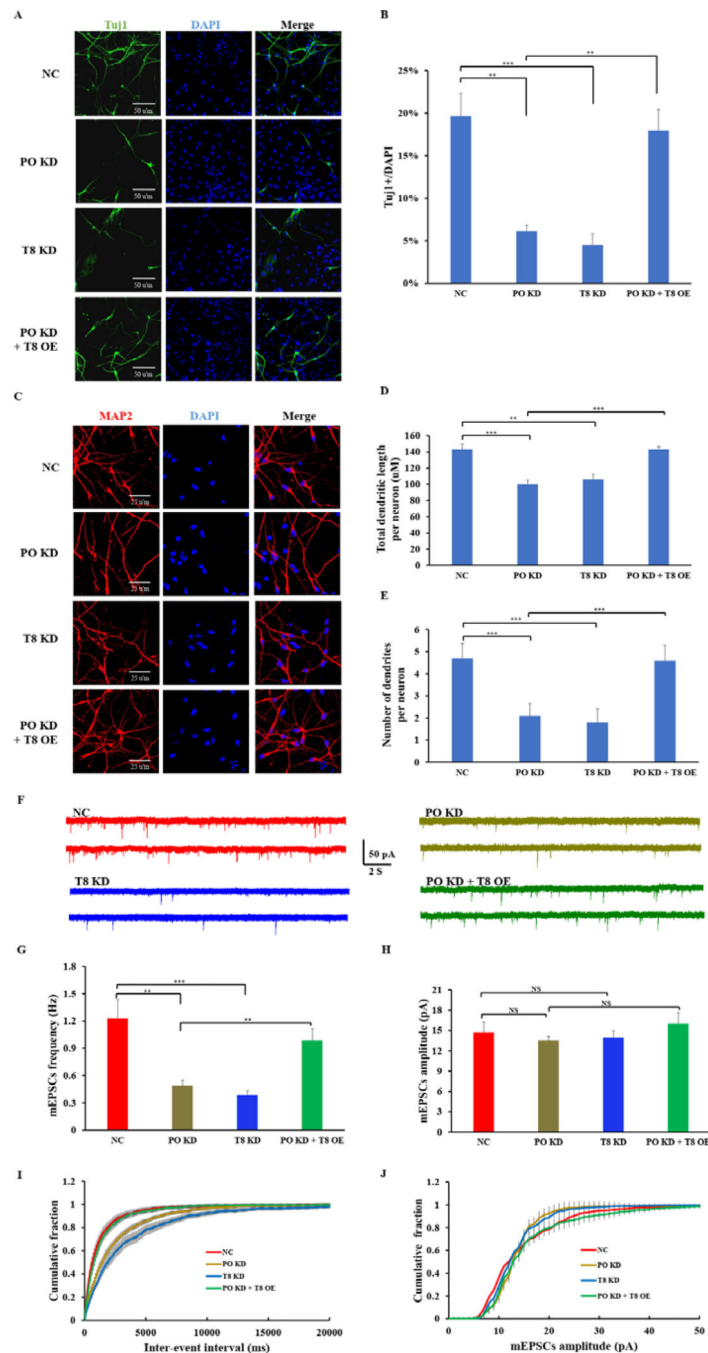
Figure 5. Suppressing *POU3F2* and *TRIM8* expression inhibited neuronal differentiation and excitatory synaptic transmission.

(A) The proportion of cells expressing Tuj1 in relation to total number of cells. *Tuj1*, a marker for staining immature neurons. NC, negative control, infection of scrambled shRNA lentivirus; PO KD, *POU3F2* knockdown, infection of sh*POU3F2*-C lentivirus; T8 KD, *TRIM8* knockdown, infection of sh*TRIM8*-C lentivirus; PO KD + T8 OE, *POU3F2* knockdown plus *TRIM8* overexpression, infection of sh*POU3F2*-C and *TRIM8* overexpression lentivirus; (B) Data quantification for (A). (C) *POU3F2* and *TRIM8* knockdown affected dendrite development. *MAP2* (microtubule associated protein 2), a

marker for staining neuronal dendrites. DAPI (4',6-diamidino-2-phenylindole), a standard DNA staining. (D) Data quantification for dendrite length. (E) Data quantification for dendrite number. All data are mean ± sd from three independent biological replicates. For each biological replicate, we designed three technical replicates. $**P < 0.01$, $***P < 0.001$, two-tailed Student's t-test. (F) Representative traces of miniature excitatory postsynaptic currents. (G and H) *POU3F2* and *TRIM8* knockdown reduced mEPSC frequency (G) without affecting mEPSC amplitude (H). 16 neurons were recorded for NC and T8 KD groups, 17 and 19 neurons were recorded for PO KD and PO KD + T8 OE groups, respectively. N = 3 independent biological experiments. (I and J) Cumulative probability plot of the inter-event interval (I) and amplitude (J).